Volume 9 | Number 4 | 28 January 2018 | Pages 779–1074

Chemical Science

rsc.li/chemical-science

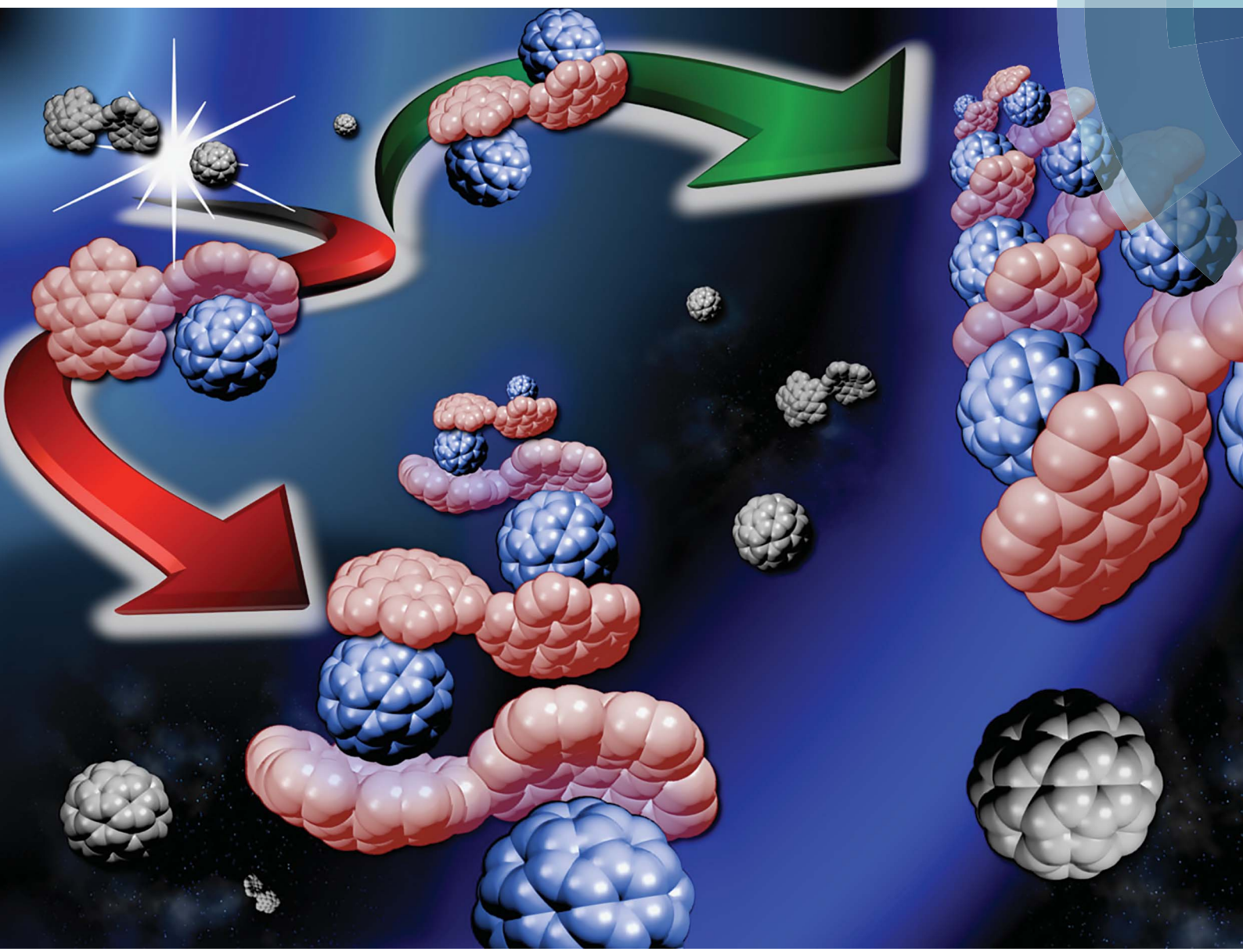

ISSN 2041-6539

ROYAL SOCIETY OF CHEMISTRY

EDGE ARTICLE
Satoru Hiroto, Hiroshi Shinokubo *et al.*
Supramolecular assemblies of a nitrogen-embedded buckybowl dimer with C_{60}

Chemical Science

EDGE ARTICLE

View Article Online
View Journal | View Issue

Cite this: *Chem. Sci.*, 2018, **9**, 819

Supramolecular assemblies of a nitrogen-embedded buckybowl dimer with C_{60}†

Hiroki Yokoi,[a] Satoru Hiroto,[a]* Daisuke Sakamaki,[b] Shu Seki[b] and Hiroshi Shinokubo[a]*

Received 15th October 2017
Accepted 20th November 2017

DOI: 10.1039/c7sc04453d

rsc.li/chemical-science

A directly connected azabuckybowl dimer was synthesized *via* a palladium-catalysed C–H/C–Br coupling. The electron-donating nature of the pyrrolic nitrogen atoms of the azabuckybowl enabled a strong complexation with pristine C_{60}. In the presence of two equivalents of C_{60}, the azabuckybowl dimer formed crystals with a 1 : 2 stoichiometry. Conversely, in diluted solution, complexes with a 1 : 1 stoichiometry of the dimer and C_{60} were detected predominantly, and these precipitated upon increasing the concentration of C_{60}. Scanning electron microscopy images of the precipitate showed fibre-like aggregates, indicating the formation of supramolecular assemblies with 1D chain structures. A variable-temperature ^{1}H NMR analysis revealed that the precipitate consists of the dimer and C_{60} in a 1 : 1 ratio.

Introduction

Supramolecular assembly is defined as higher-order aggregates constructed from two or more components, in which the molecules interact by non-covalent interactions such as hydrogen bonding, metal coordination, or hydrophobic interactions.[1] As these interactions are much weaker than covalent bonds, cleavage of the aggregates easily occurs by adjusting the temperature or concentration, which regenerates the corresponding monomers. Due to this flexibility, supramolecular polymers are expected to act as stimulus-responsive materials.[2] Among all the research in this field, supramolecular polymers with fullerenes based on host–guest interactions have been extensively studied in recent years (Fig. 1).[3–6] Previous studies have often employed molecular tweezers hosts to ensure strong binding with C_{60} derivatives. These strategies require a C_{60} dimer (type a; Fig. 1) or a functionalized C_{60} bearing a binding site (type b; Fig. 1). However, supramolecular polymerization with pristine C_{60} remains a challenge because two binding units of the molecular tweezers would be needed to capture one C_{60} molecule.[7] Consequently, stronger yet sterically less-demanding host molecules are required.

Buckybowls are bowl-shaped π-conjugated molecules, for which sumanenes and corannulenes are representative examples.[8,9] Such curved polycyclic aromatic hydrocarbons have been used for the recognition of fullerenes, given that the concave surface of the former efficiently overlaps with the convex surface of the latter.[10] And it is exactly for this reason that extensive research on assemblies of buckybowls with fullerenes has been carried out.[11] However, due to the poor electron-donating nature of these buckybowls,[12] their binding ability is usually insufficient to construct large supramolecular assemblies.

Recently, the group of Nozaki and our own group have independently succeeded in the synthesis of nitrogen-embedded buckybowls such as penta-*peri*-pentabenzoazacorannulene **1** (Chart 1).[13] Due to the electron-donating nature of the pyrrolic nitrogen atom, buckybowl **1** exhibited a large association constant with C_{60} in solution. The binding constant of **1** was 3800 M^{-1} in 1,2-dichlorobenzene, which is a top-class value reported for a bowl-shaped molecule. This result suggests that **1** could be used as a new building block for supramolecular assemblies with C_{60}.

Herein, we disclose the synthesis of buckybowl dimer **2** as a host molecule for pristine C_{60}. Owing to its two binding sites,

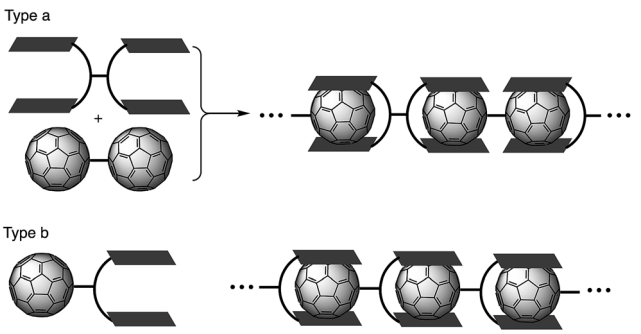

Fig. 1 Supramolecular polymerization of C_{60} derivatives.

[a]*Department of Molecular and Macromolecular Chemistry, Graduate School of Engineering, Nagoya University, Furo-cho, Chikusa-ku, Nagoya, Aichi 464-8603, Japan. E-mail: hiroto@chembio.nagoya-u.ac.jp; hshino@chembio.nagoya-u.ac.jp*

[b]*Department of Molecular Engineering, Graduate School of Engineering, Kyoto University, Kyoto daigaku Katsura, Nishikyo-ku, Kyoto 615-8510, Japan*

† Electronic supplementary information (ESI) available. CCDC 1579079 and 1579080. For ESI and crystallographic data in CIF or other electronic format see DOI: 10.1039/c7sc04453d

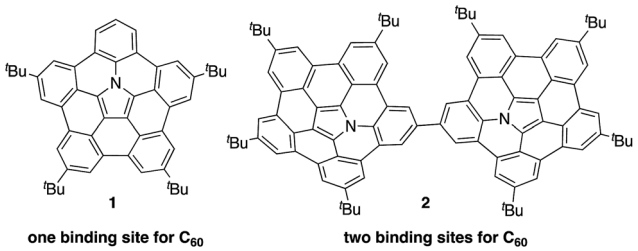

Chart 1 Azabuckybowl **1** and linked azabuckybowl dimer **2**.

dimer **2** was expected to form complexes with C_{60} in either a 1 : 1 or 1 : 2 ratio. We discovered that **2** acts as a concentration-dependent fullerene host, showing drastic morphological changes in the solid state depending on the number of C_{60} molecules that are contained within the structure. In particular, 1D-chain fibre aggregates consisting of **2** and C_{60} were obtained.

Results and discussion

Synthesis and characterization

In our previous work, **1** was synthesized *via* the Pd-mediated C–H/C–Br coupling of tribrominated precursor **3** using an excess of palladium(II) acetate and tricyclohexylphosphonium tetrafluoroborate. Interestingly, the use of catalytic amounts of these reagents provided the linked azabuckybowl dimer **2** in 31% yield (Scheme 1). The structure of **2** was characterized by NMR spectroscopy and mass spectrometry. The parent mass ion peak of **2** was observed at m/z = 1321.7303, which confirms its dimeric structure. The ^{1}H NMR spectrum of **2** exhibited five singlet peaks in the aromatic region, consistent with a symmetric structure for **2** (Fig. S1†). The downfield shifts of the H^a protons (Scheme 1) in **2** compared to those in **1** indicate a deshielding effect by the second azabuckybowl unit. In addition, the ^{13}C NMR spectrum exhibited 18 peaks assignable to sp^2-carbons, which suggests a conformation with C_{2v} symmetry (Fig. S2†).

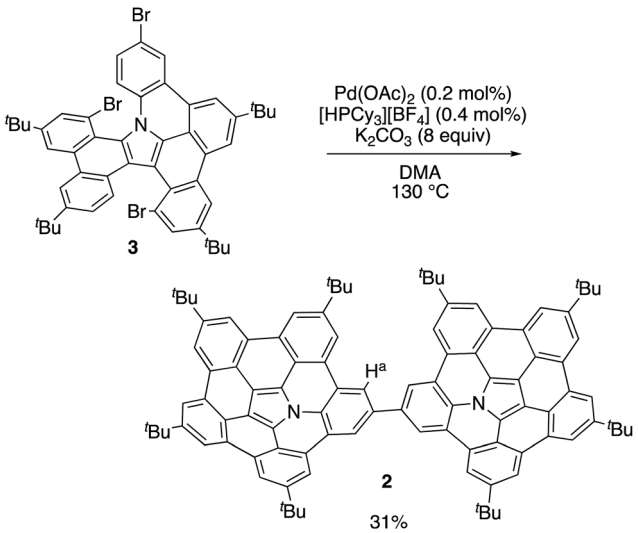

Scheme 1 Synthesis of directly linked azabuckybowl dimer **2**.

Optical and electrochemical properties

Fig. 2 shows the UV-vis absorption and emission spectra of **1** and **2** in CH_2Cl_2. Compared to the spectrum of **1**, the lowest-energy band of **2** was red-shifted from 472 nm to 495 nm, which indicates the presence of electronic communication between the two azabuckybowl units through the covalent bond. The emission band of **2** was observed at 517 nm with a quantum yield of 0.17, which is almost identical to that of **1**. The electrochemical properties of **2** were investigated by cyclic voltammetry (Fig. S3†), where **2** exhibited a lower oxidation potential (0.18 V) than **1** (0.20 V), commensurate with higher electron-donating properties for **2**.

Titration experiments between 2 and C_{60}

In order to examine the binding ability of **2** toward C_{60} in solution, we carried out titration experiments under diluted conditions (c = 1.3 × 10^{-5} M^{-1}) (Fig. 3). The titration was conducted in 1,2-dichlorobenzene and monitored by UV-vis-NIR absorption spectroscopy. Upon addition of a solution of C_{60} to a solution of **2**, an absorption band around 800 nm appeared, which is similar to the behaviour of **1**. The Job's plot for the absorbance at 800 nm indicated the predominant formation of 1 : 1 complexes in solution (Fig. S4†). A nonlinear curve fitting based on a 1 : 1 binding afforded an association constant of 7.8 × 10^3 M^{-1}, which is higher than that of **1** (K_a = 3.8 × 10^3 M^{-1}). This result corroborates the superior electron-donating nature of **2** relative to that of **1**. It should also be noted that the binding constant reached 1.0 × 10^5 M^{-1} in toluene (Fig. S5 and S6†). Such solvent-dependent association constants should probably be attributed to the different solvophobicity of the fullerene in each solvent.[14]

X-ray crystal structure and charge-carrier mobility

Fortunately, we obtained single co-crystals of **2** and C_{60} that were suitable for an X-ray diffraction analysis, which were prepared by vapour diffusion of acetonitrile into a toluene

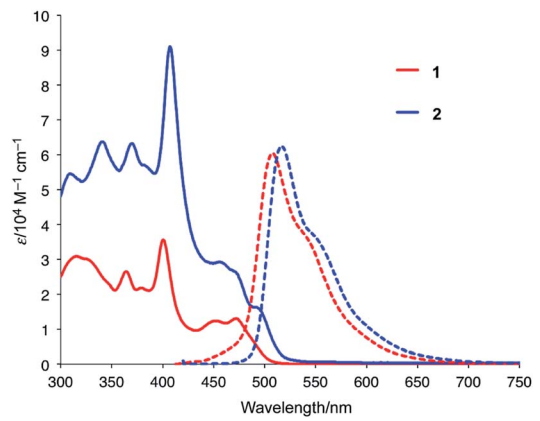

Fig. 2 UV-vis absorption and emission spectra of **1** and **2** in CH_2Cl_2.

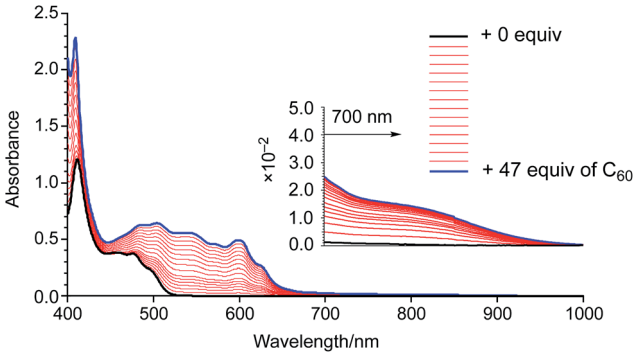

Fig. 3 UV-vis-NIR absorption spectra of a 1,2-dichlorobenzene solution of **2** upon addition of 0–47 equiv. of C_{60}.

solution of a mixture of **2** and C_{60} (Fig. 4).[15] In these crystals, the two azabuckybowl units face in opposite directions, reflected in the tilt angle (50.1°) between the two buckybowl units around the central bond. The C_{60} molecules are coordinated to the azabuckybowl units in a concave–convex fashion, resulting in a 1 : 2 ratio in the crystal. Between the centroid of the pyrrole ring to the closest surface of the C_{60} molecules, distances of 3.28 and 3.29 Å were measured. Such short distances indicate the existence of strong electronic interactions between **2** and C_{60} in the solid state. The packing structure is shown in Fig. 4b.

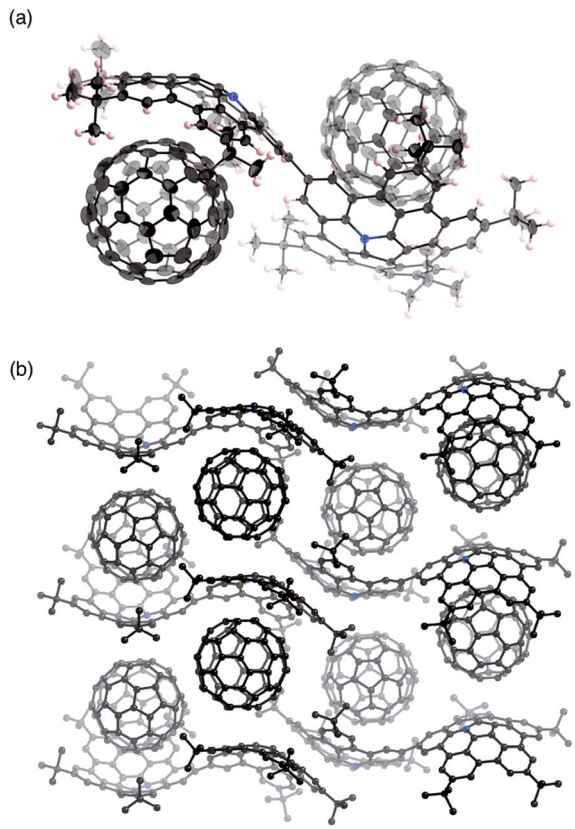

Fig. 4 Molecular structure of **2**·C_{60} in the crystal: (a) side view and (b) packing structure. Solvent molecules (toluene) have been omitted for clarity. The thermal ellipsoids are scaled at 50% probability level.

Similar to **1**·C_{60}, **2** and the C_{60} molecules present segregate stacking (Fig. S7†). The photo-induced transient conductivity of **2** and **2**·C_{60} was determined by flash-photolysis time-resolved microwave conductivity (FP-TRMC) measurements.[16] The carrier mobility of the **2**·C_{60} crystals (2.0×10^{-4} cm^2 V^{-1} S^{-1}) is approximately by one order of magnitude higher than that of **2** (Fig. S8†). The carrier mobility of the **2**·C_{60} crystals was similar to that of **1**·C_{60}, indicating a similar charge-separation state between C_{60} and the azabuckybowl unit in the crystal.

Supramolecular assembly of 2 with C_{60}

To uncover the different binding ratios of **2** with C_{60} in solution and the crystalline state, we carried out titration experiments in toluene at 20 °C, which were monitored by ^{1}H NMR spectroscopy (Fig. 5). With increasing amount of C_{60}, the spectral shape of the signal peaks became broader and the peak intensities decreased. Notably, a precipitate was formed in the presence of 1.0 equiv. or less of C_{60}. This phenomenon was not observed in the case of **1**, for which a clear solution was obtained in the presence of C_{60}. To clarify this phenomenon, we performed diffusion-ordered two-dimensional NMR spectroscopy (DOSY) experiments.[17] The diffusion coefficient (D) determined for **2** (6.83×10^{-10} m^2 s^{-1}) decreased by 15% (5.80×10^{-10} m^2 s^{-1}) in the presence of 0.5 equiv. of C_{60}. In contrast, a reduction of only 2% was observed in the case of **1** (Fig. S9†). This drop in the D value of **2** indicates the formation of larger structures.

The macroscopic structure of the precipitate formed in the presence of C_{60} was investigated by scanning electron microscopy (SEM). For that purpose, samples were prepared by drop-casting toluene solutions onto silicon wafers. Fig. 6 displays the SEM images of **2** and **2** with 1.0 equiv. of C_{60}. In the precipitate, fibre-like structures were observed, while a film-like morphology was observed for **2**, similar to the case of **1** with C_{60} (Fig. S10†). These results indicate that **2** and C_{60} assemble into

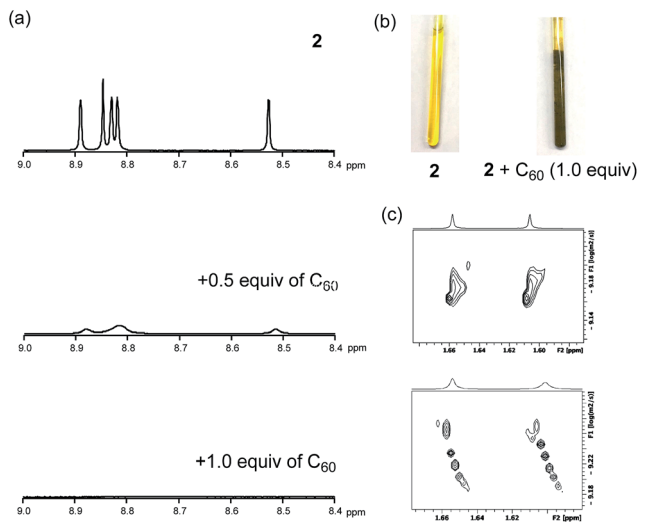

Fig. 5 ^{1}H NMR titration experiments of **2** in toluene-d_8. (a) ^{1}H NMR spectra of **2** (0.52 mM) with increasing amounts of C_{60}, (b) photographs of samples of **2** and **2** + C_{60}, and (c) DOSY measurements of **2** and **2** + C_{60}.

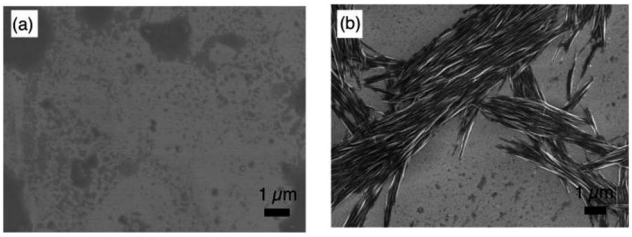

Fig. 6 SEM images of (a) **2** and (b) **2** with 1.0 equiv. of C_{60}.

a one-dimensional (1D) supramolecular structure. Based on comparative experiments with **1**, it can be concluded that the dimeric structure plays an important role in the formation of supramolecular assemblies.

The stoichiometric ratio between **2** and C_{60} in the precipitate was determined by variable-temperature ^{1}H NMR measurements in toluene-d_8 (Fig. 7). We conducted experiments at low temperature to accelerate the assembly process. At −40 °C, the broad spectrum of **2** in the presence of 0.5 equiv. of C_{60} became very similar to the spectrum of **2**, which exhibited sharp peaks. Using 1,1,2,2-tetrachloroethane as the internal standard revealed that ∼50% the original amount of **2** remained in solution (Fig. S11†). Consequently, we concluded that the precipitate consists of **2** and C_{60} in a 1 : 1 ratio. Notably, peaks in the aromatic region appeared upon addition of 2.0 equiv. of C_{60}, and these are completely different from those observed for **2** (see also Fig. S12†).

The composition of the fibres was further analysed by MALDI-TOF mass spectrometry (Fig. 8). The spectrum exhibited several intense peaks at regular intervals. The gaps between the peaks correspond to the molecular weight of **2** or C_{60}. The largest observable peak was at M_w = 13 kDa, corresponding to a 6 : 6 complex of **2** and C_{60}. In their entirety, the NMR, SEM, and MS analyses allow the conclusion that the fibres consist of a 1D chain-like assembly of **2** and C_{60} in a 1 : 1 ratio.

To elucidate more structural details of the fibres, we performed a powder X-ray diffraction (XRD) analysis (Fig. S13†), which exhibited two broad peaks at $2\theta = 2.44°$ (36.2 Å) and 5.00° (17.7 Å). The spectral pattern of the fibres is thus inconsistent with that of the single crystal of **2**·C_{60}, suggesting the formation of a different packing structure. On the other hand, a powdered sample of **2** showed weak and broad reflections at 2θ = 4.94° (17.9 Å) and 6.18° (14.3 Å), indicating the lack of structural regularity in **2**.

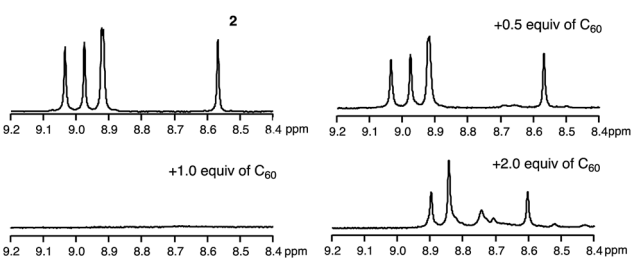

Fig. 7 ^{1}H NMR spectra of **2** and **2** + C_{60} at −40 °C in toluene-d_8.

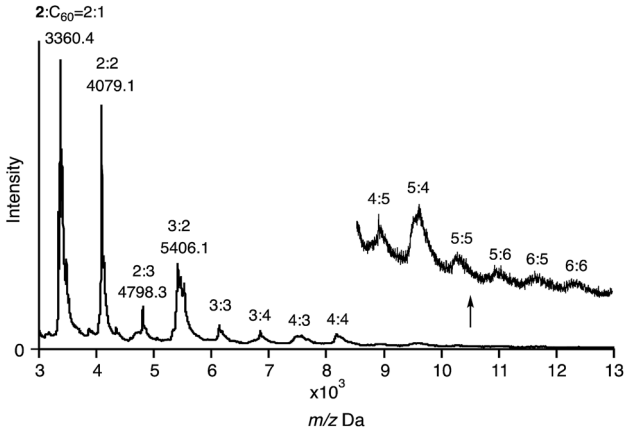

Fig. 8 MALDI-TOF MS spectrum of **2** with 1.0 equiv. of C_{60} (matrix: *trans*-2-[3-(4-*tert*-butylphenyl)-2-methyl-2-propenylidene]malononitrile; DCTB).

Fig. 9 shows the UV-vis-NIR absorption of **2** and its inclusion complexes in the solid state. In contrast to **2**, the **2**·C_{60} crystal exhibits a broad absorption band around 850 nm, which was characterized as a charge transfer (CT) band. The fibre aggregates also exhibit an NIR absorption band, indicating similar concave–convex binding between **2** and C_{60} in the structure. However, the intensity of this band was higher for the fibre than for the crystal, suggesting different packing structures for these two samples.

Two binding modes are possible for the association of **1** with C_{60}. One is a 1 : 1 concave–convex complex and the other one involves the formation of a 1 : 2 sandwich-type complex. We anticipated that these two binding modes should result in different UV-vis-NIR absorption features in the solid state. Fortunately, by changing the solvents used for recrystallization from methanol/toluene to hexane/chloroform, a 2 : 1 complex of **1** and C_{60} was obtained.[18] The single-crystal X-ray diffraction analysis of the complex unambiguously revealed a sandwich-type structure, in which two azabuckybowl molecules cooperatively capture a C_{60} molecule by concave–convex interactions (Fig. 10). In addition, we recorded the solid-state UV-vis-NIR

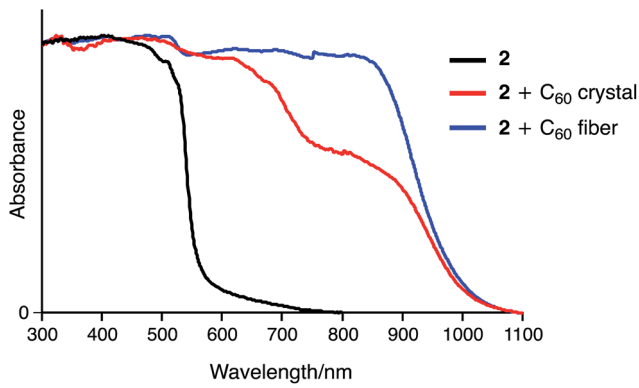

Fig. 9 Solid-state UV-vis-NIR absorption spectra of **2**, **2** + C_{60} crystal, and **2** + C_{60} fibre (spectra were normalized at 300 nm).

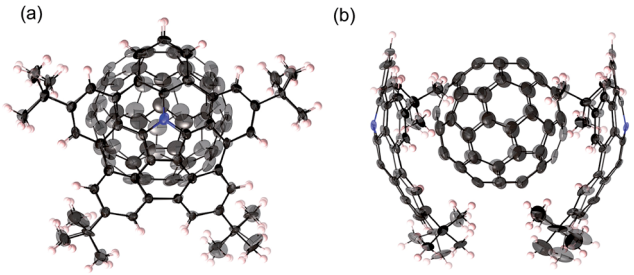

Fig. 10 Molecular structure of $\mathbf{1}_2\cdot C_{60}$ in the crystal: (a) side view and (b) packing structure. The thermal ellipsoids are scaled at 50% probability level.

absorption spectra of the crystals for both 1 : 1 and 2 : 1 binding modes (Fig. 11). Both 1 : 1 and 2 : 1 complexes exhibit CT absorption bands around 850 nm. Notably, the absorption intensity at this wavelength is higher for the 2 : 1 complex than for the 1 : 1 complex. The theoretical calculations by the TD-DFT method also support these experimental results. The simulated absorption bands assigned to the CT transitions are significantly large in the 2 : 1 complex as compared to that in the 1 : 1 complex (Fig. S14†). Such an enhancement of the CT band was also observed in the absorption spectrum of **2** + C_{60}. This spectral similarity strongly indicates a sandwich-type binding mode in the $\mathbf{2}\cdot\mathbf{C_{60}}$ fibres.

Plausible structures and mechanism of supramolecular assembly

Scheme 2 illustrates the plausible association mechanism of **2** with C_{60}. In the initial binding step, a 1 : 1 complex between **2** and C_{60} should be formed. Binding to the second C_{60} molecule would be weaker due to the reduced electron-donating ability of the other azabuckybowl unit after binding the first electron-deficient C_{60}.[19] Consequently, the 1 : 1 complex is obtained predominant in dilution. The 1 : 1 complexes interact with each other under more concentrated conditions to form fibres by sandwich-type binding, which are insoluble in organic solvents. We optimized the structure of the 1D chain-like arrangement using PM6 semi-empirical calculations (Fig. S15†). The calculated interplanar spacing (17.8 Å) is in good agreement with the XRD results (17.7 Å). Further addition of C_{60} to the fibres induces cleavage of the polymer chain to form soluble fragments, as detected by ^{1}H NMR spectroscopy.

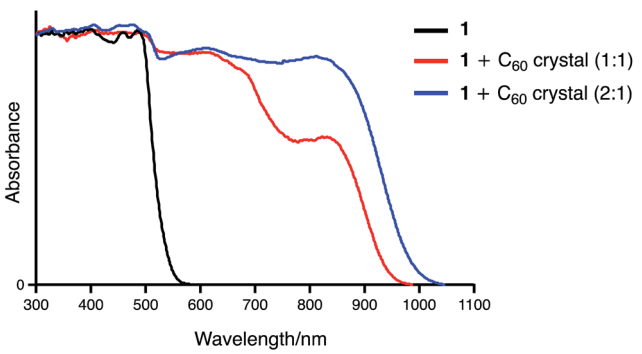

Fig. 11 Solid state UV-vis-NIR absorption spectra of **1**, $\mathbf{1}\cdot C_{60}$, and $\mathbf{1}_2\cdot C_{60}$ (spectra were normalized at 300 nm).

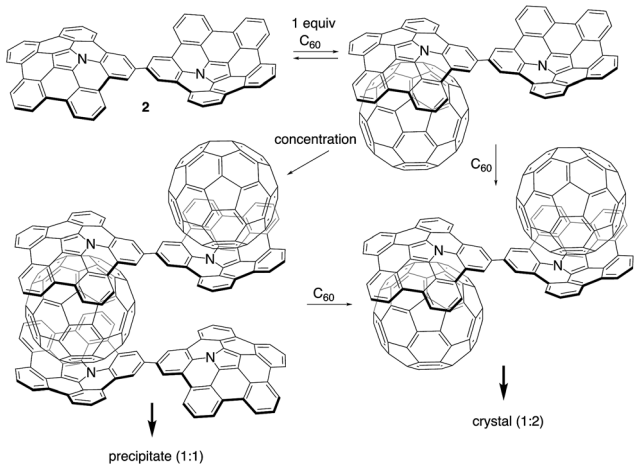

Scheme 2 Plausible association mechanism for **2** in the presence of increasing amounts of C_{60} (*tert*-butyl groups are omitted for clarity).

Conclusions

In summary, we have synthesized a directly linked azabuckybowl dimer from a tribrominated monomeric precursor. The dimer exhibits strong 1 : 1 complexation with C_{60} in solution. Segregated stacks of **2** and C_{60} were observed in the crystalline state, suggesting efficient photo-excited charge-carrier mobility. Under concentrated conditions, **2** and C_{60} form 1D chain supramolecular assemblies with a fibrous structure. The present results demonstrate that an electron-donating bowl-shaped π-conjugated molecule can serve as a binding motif for pristine C_{60} for the construction of supramolecular assemblies based on strong donor–acceptor interactions.

Conflicts of interest

There are no conflicts for declare.

Acknowledgements

We would like to acknowledge Prof. Takahiro Seki and Dr Mituo Hara (Nagoya University) for their help with the powder X-ray diffraction measurements. We also thank Dr Ichiro Hisaki (Osaka University) for his help with the single-crystal X-ray diffraction analysis of $\mathbf{2}\cdot\mathbf{C_{60}}$. This work was supported by JSPS KAKENHI grants JP16H06031, JP26102003, and JP15H00731, as well as the Program for Leading Graduate Schools "Integrative Graduate Education and Research in Green Natural Sciences" from MEXT (Japan). S. H. expresses his gratitude for financial support from the Tokuyama Science Foundation. Y. H. acknowledges a grant-in-aid for JSPS Research Fellows (JP15J10528).

Notes and references

1 (*a*) L. Brunsveld, B. J. B. Folmer, E. W. Meijer and R. P. Sijbesma, *Chem. Rev.*, 2001, **101**, 4071; (*b*) T. F. A. De Greef, M. M. J. Smulders, M. Wolffs, A. P. H. J. Schenning, R. P. Sijbesma and E. W. Meijer, *Chem. Rev.*, 2009, **109**, 5687; (*c*) L. Yang, X. Tan, Z. Wang and X. Zhang, *Chem. Rev.*, 2015, **115**, 7196.

2 (*a*) X. Yan, F. Wang, B. Zheng and F. Huang, *Chem. Soc. Rev.*, 2012, **41**, 6042; (*b*) X. Ma and H. Tian, *Acc. Chem. Res.*, 2014, **47**, 1971.

3 F. Giacalone and N. Martín, *Chem. Rev.*, 2006, **106**, 5136.

4 *Supramolecular Chemistry of Fullerenes and Carbon Nanotubes*, ed. N. Martín and J.-F. Nierengarten, Wiley-VCH, Weinheim, 2012.

5 (*a*) G. Fernández, E. M. Pérez, L. Sánchez and N. Martín, *Angew. Chem., Int. Ed.*, 2008, **47**, 1094; (*b*) G. Fernández, E. M. Pérez, L. Sánchez and N. Martín, *J. Am. Chem. Soc.*, 2008, **130**, 2410.

6 (*a*) T. Hirao, M. Tosaka, S. Yamago and T. Haino, *Chem.–Eur. J.*, 2014, **20**, 16138; (*b*) T. Haino, Y. Matsumoto and Y. Fukazawa, *J. Am. Chem. Soc.*, 2005, **127**, 8936; (*c*) H. Isla, E. M. Pérez and N. Martín, *Angew. Chem., Int. Ed.*, 2014, **53**, 5629.

7 (*a*) Y. Liu, H. Wang, P. Liang and H.-Y. Zhang, *Angew. Chem., Int. Ed.*, 2004, **43**, 2690; (*b*) Y. Liu, Y.-W. Yang, Y. Chen and H.-X. Zou, *Macromolecules*, 2005, **38**, 5838; (*c*) M. Shirakawa, N. Fujita and S. Shinkai, *J. Am. Chem. Soc.*, 2003, **125**, 9902; (*d*) M. Fathalla, S.-C. Li, U. Diebold, A. Alb and J. Jayawickramarajah, *Chem. Commun.*, 2009, 4209.

8 *Fragments of Fullerenes and Carbon Nanotubes: Designed Synthesis, Unusual Reactions, and Coordination Chemistry*, ed. M. A. Petrukhina and L. T. Scott, Wiley, Hoboken, 2012.

9 (*a*) Y.-T. Wu and J. S. Siegel, *Chem. Rev.*, 2006, **106**, 4843; (*b*) H. Sakurai, T. Daiko and T. Hirao, *Science*, 2003, **301**, 1878; (*c*) W. E. Barth and R. G. Lawton, *J. Am. Chem. Soc.*, 1966, **88**, 380.

10 T. Kawase and H. Kurata, *Chem. Rev.*, 2006, **106**, 5250.

11 (*a*) L. N. Dawe, T. A. AlHujran, H.-A. Tran, J. I. Mercer, E. A. Jackson, L. T. Scott and P. E. Georghiou, *Chem. Commun.*, 2012, **48**, 5563; (*b*) A. S. Filatov, M. V. Ferguson, S. N. Spisak, B. Li, C. F. Campana and M. A. Petrukhina, *Cryst. Growth Des.*, 2014, **14**, 756; (*c*) S. Mizyed, P. E. Georghiou, M. Bancu, B. Cuadra, A. K. Rai, P. Cheng and L. T. Scott, *J. Am. Chem. Soc.*, 2001, **123**, 12770; (*d*) A. Sygula, F. R. Fronczek, R. Sygula, P. W. Rabideau and M. M. Olmstead, *J. Am. Chem. Soc.*, 2007, **129**, 3842; (*e*) M. Yanney, F. R. Fronczek and A. Sygula, *Angew. Chem., Int. Ed.*, 2015, **54**, 11153; (*f*) C. M. Álvarez, L. A. García-Escudero, R. García-Rodríguez, J. M. Martín-Álvarez, D. Miguel and V. M. Rayón, *Dalton Trans.*, 2014, **43**, 15693; (*g*) P. L. A. Kuragama, F. R. Fronczek and A. Sygula, *Org. Lett.*, 2015, **17**, 5292.

12 (*a*) J. Janata, J. Gendell, C.-Y. Ling, W. E. Barth, L. Backes, H. B. Mark and R. G. Lawton, *J. Am. Chem. Soc.*, 1967, **89**, 3056; (*b*) T. J. Seiders, K. K. Baldridge, J. S. Siegel and R. Gleiter, *Tetrahedron Lett.*, 2000, **41**, 4519; (*c*) P. Zanello, S. Fedi, F. F. de Biani, G. Giorgi, T. Amaya, H. Sakane and T. Hirao, *Dalton Trans.*, 2009, 9192.

13 (*a*) H. Yokoi, Y. Hiraoka, S. Hiroto, D. Sakamaki, S. Seki and H. Shinokubo, *Nat. Commun.*, 2015, **6**, 8215; (*b*) S. Ito, Y. Tokimaru and K. Nozaki, *Angew. Chem., Int. Ed.*, 2015, **54**, 7256.

14 V. H. Le, M. Yanney, M. McGuire, A. Sygula and E. A. Lewis, *J. Phys. Chem. B*, 2014, **118**, 11956.

15 X-ray crystallographic data for **2·C$_{60}$**: formula: $C_{247.73}H_{123.18}N_2$, M_w = 3127.42, monoclinic, space group: $P2_1/c$, a = 13.1579(2) Å, b = 37.8588(7) Å, c = 30.9277(5) Å, β = 96.192(2)°, V = 15316.5(4) Å^3, Z = 4, D_c = 1.356 g cm^{-3}, R_1 = 0.1090($I > 2\sigma(I)$), wR_2 = 0.3338 (all data), GOF = 1.085. CCDC number: 1579079.

16 S. Seki, A. Saeki, T. Sakurai and D. Sakamaki, *Phys. Chem. Chem. Phys.*, 2014, **16**, 11093.

17 C. S. Johnson Jr, *Prog. Nucl. Magn. Reson. Spectrosc.*, 1999, **34**, 203.

18 X-ray crystallographic data for **1$_2$·C$_{60}$**: formula: $C_{320}H_{188}N_4$, M_w = 4088.73, monoclinic, space group: $P2_1$, a = 17.0175(8) Å, b = 28.9186(13) Å, c = 22.7929(10) Å, β = 100.4840(10), V = 11029.6(9) Å^3, Z = 2, D_c = 1.231 g cm^{-3}, R_1 = 0.0969($I > 2\sigma(I)$), wR_2 = 0.2627 (all data), GOF = 1.077. CCDC number: 1579080.

19 A negative allosteric effect of C_{60} has been reported; see: (*a*) K. Miki, T. Matsushita, Y. Inoue, Y. Senda, T. Kowada and K. Ohe, *Chem. Commun.*, 2013, **49**, 9092; (*b*) H. Sato, K. Tashiro, H. Shinmori, A. Osuka, Y. Murata, K. Komatsu and T. Aida, *J. Am. Chem. Soc.*, 2005, **127**, 13086; (*c*) L. Moreira, J. Calbo, J. Aragó, B. M. Illescas, I. Nierengarten, B. Delavaux-Nicot, E. Ortí, N. Martín and J.-F. Nierengarten, *J. Am. Chem. Soc.*, 2016, **138**, 15359.